ACS OMEGA

Open Access

http://pubs.acs.org/journal/acsodf

Article

Influence of Air Volume and Temperature in the Air Inlet Tunnel on the Characteristics of Dust Movement

YeMing Zhu,* Tao Chen, ShuTang Sun,* Ying Ji, Dong Zhao, DaJie Zhuang, YiRen Lian, Yu Rong, Jin Yan, and HongChao Sun

Cite This: *ACS Omega* 2024, 9, 866−878

Read Online

ACCESS | Metrics & More | Article Recommendations

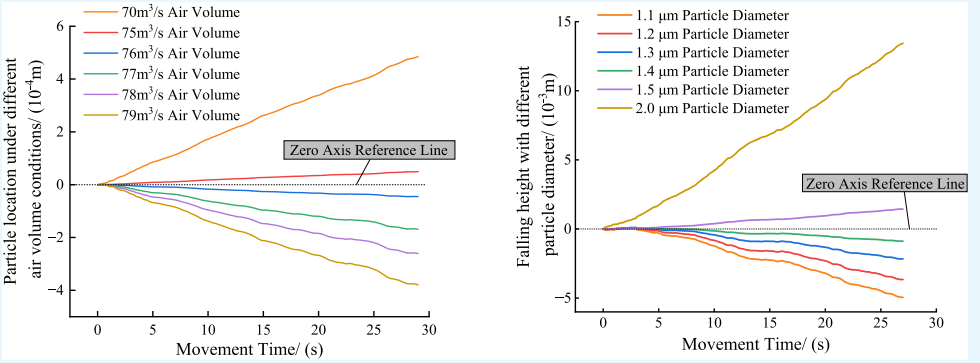

ABSTRACT: In order to clarify the movement characteristics of dust particles in the intake tunnel and improve the underground intake tunnel environment, the main intake tunnel of Wulihou Coal Mine was taken as the engineering background, the COMSOL simulation software was adopted to establish a model, the influence of air volume and temperature on dust movement characteristics was studied, and the critical air volume and particle size of dust at room temperature were determined. The results show that with the ventilation air volume being the same, when the dust reaches the exit of the tunnel, its falling height is positively correlated with the particle size. When the dust particle size is the same, the height of the dust falling is negatively correlated with the ventilation air volume. As the particle size of dust increases, the impact of changes in air volume on its movement decreases and the trajectory of dust movement gradually becomes consistent. The height of dust falling is negatively correlated with the air flow temperature. Therefore, when other factors remain unchanged, dust pollution in the tunnel is relatively severe during the day and the dust concentration in the tunnel is higher in summer. The critical air volume for dust emission in the intake tunnel of Wulihou Coal Mine is 75.84 m^3/s, corresponding to a central wind speed of 5.29 m/s in the tunnel. The critical particle size for dust emission is 1.4 μm.

1. INTRODUCTION

In China, coal mining is mainly conducted in an underground confined space. If the dust generated in the coal mining process is not removed in time, it will cause dust explosion,[1] industrial accidents, occupational diseases, and other hazards; therefore, experts attach great importance to mine dust control.[2] With the rapid development of computer software, a large number of numerical simulations have been used to study the dust movement in coal mine tunnels.[3−7] Mo et al. analyze the characteristics of air flow transport and dust pollution on a fully mechanized top-coal caving face at different inlet wind velocities by using a numerical simulation experiment, and the best wind velocity for dust suppression is obtained.[8] Tallón-Ballesteros A J. studied the wind flow field and dust transport law of the comprehensive mining work surface, and the comprehensive mining working surface under different inlet wind speed conditions was simulated and analyzed by Fluent. The results show that due to the existence of the high-speed wind flow belt, dust is mainly distributed near the downwind side working surface.[9] Wang measured the dust in the laboratory and obtained the dust concentration, mixed dust quality, and particle size distribution of different particles of dust at different heights along the roadway under different wind speeds. The results showed that on the same section, the dust concentration is directly proportional to the distance from the roof.[10] Zhou et al. combined on-site application with numerical simulation, and the results showed that the ventilation air flow gradually stabilizes, large particle

Received: September 11, 2023
Revised: November 12, 2023
Accepted: November 14, 2023
Published: December 4, 2023

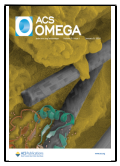

https://doi.org/10.1021/acsomega.3c06816
ACS Omega 2024, 9, 866−878

size dust particles continue to settle, and most of the suspended dust particles in the air flow have particle sizes less than 40 μm.[11] Jiang et al. established a mathematical model for the distribution of mobile dust diffusion. The results showed that during the polishing operation stage, the dust mass concentration gradually decreases with time, and the dust cloud drifts downstream and spreads around, increasing its influence radius. The dust mass concentration increases with the increase of the source intensity, and the source intensity has no effect on the position of the peak dust mass concentration. The smaller the average particle size of the dust, the higher the dust mass concentration. The higher the wind speed, the lower the overall dust concentration.[12] Hu et al. calculated the movement process of airborne dust in the comprehensive excavation face based on the theory of gas−solid two-phase flow, and elaborated on the characteristics of gas−solid two-phase flow in the high gas coal seam excavation face.[13] Wang used numerical simulation to identify the impact of the flow field on dust transport and settlement when using pressure ventilation in excavation tunnels: large particle dust deposition and accumulation occur within 3−5 m from the end of the excavation face. As the distance between the end of the working face increases, the particle size of the settled dust gradually decreases and the distribution becomes more uniform.[14] At present, the dust removal methods of coal mining face include spray dust reduction,[15] foam dust removal,[16] ventilation dust removal,[17] and other methods, but there are relatively few studies on the coupling effect of temperature and wind speed on dust movement.

To sum up, the analysis of dust movement characteristics at home and abroad mainly focuses on the microscopic study of local areas,[18,19] especially the integrated excavation face and the coal face,[20] but there are few reports on the dust distribution in the air inlet roadway of coal mine. Therefore, in this paper, the Wulihou tunnel was taken as the engineering background, the dust movement characteristics from the aspects of ventilation air volume and air flow temperature were studied, and the influence rule of air flow temperature on dust movement characteristics was revealed. The simulation results of the influence of air volume show that when the ventilation air volume in the inlet tunnel is the same, the height of dust falling at the outlet of the tunnel is positively correlated with its particle size. When the dust particle size is the same, there is a negative correlation between the height of dust falling and the ventilation air flow during the same movement time. The simulation results of temperature impact analysis show that the falling height of dust with the same particle size in the tunnel is negatively correlated to the air flow temperature, and the change in dust falling height caused by unit temperature change is positively correlated to the air flow temperature.

2. MODEL DESCRIPTION

2.1. Model Theory. In this paper, the Euler−Lagrange method was used to establish the mathematical model of dust movement. Due to the complex field conditions in an underground coal mine, the following reasonable simplification is made for the simulation calculation domain of dust movement in roadways in order to facilitate the establishment of models and grid division. First, the following assumptions are made for the simulation calculation domain:[21]

(1) Do not consider the influence of the cable and other debris in the tunnel on the air flow;
(2) Dust particles are uniform spheres;
(3) Do not consider the interaction between dust and condensation phenomenon;
(4) The fluid is homogeneous and incompressible;
(5) All of the dust flowing out of the air flow stays at the outlet;
(6) The air volume affects the ambient temperature T = 20 °C and the relative humidity φ = 0.6 in the model;
(7) There is no strong heat source inside and at the boundary of the fluid. Heat conduction is ignored in the model affected by air volume, while heat conduction is turned on in the model affected by temperature;
(8) Air leakage inside the confined space is not considered.

Dust is affected by[22,23] gravity, drag force, pressure gradient force, Safman lift force, additional mass force, and other forces during its movement. Generally, Brownian force has a great effect on fine particles with a particle size less than 0.1 μm, and this force is not considered when the particle size is larger than 0.5 um. The relative effects of other forces such as the Magnus force and Bassett force are too small to be considered in this paper. In addition, the thermal swimming force should be considered in the temperature effect model. In this simulation, a three-dimensional steady-state incompressible N−S equation is used to describe the simulation,[24,25] and the solution is solved by the standard k-ε turbulence model. The model of the influence of wind volume ignores heat conduction and only considers momentum transmission.[26]

2.2. Wind Velocity Distribution Function of Roadway Section. After revising and redefining Prandte's mixing length theory, Ji deduced that the air flow velocity distribution function in roadway is as follows:[27]

$$\overline{u} = \left(1 - \frac{16}{15}\frac{1}{k}\sqrt{\frac{\lambda}{8}} + \frac{2}{k}\sqrt{\frac{\lambda}{8}}\sqrt{1 - \frac{r}{r_0}}\right)\overline{u}_{\mathrm{m}} \tag{1}$$

In the equation, k is the experimental coefficient; λ is the friction resistance coefficient; $\overline{u}_{\mathrm{m}}$ is the average wind speed of the roadway section, m/s; r_0 is the distance from the shaft line of roadway to the farthest wall surface, m; and r is the distance between the axis line of roadway and this point, m.

According to Nikolaze's experimental results, the k value of rough wall surface is 0.4,[28] and by substituting roadway friction resistance $\alpha = \frac{\lambda}{8}\rho$[29] and k = 0.4 into eq 1, we can get

$$\overline{u} = \left(1 - \frac{8}{3}\sqrt{\frac{\alpha}{\rho}} + 5\sqrt{\frac{\alpha}{\rho}}\sqrt{1 - \frac{r}{r_0}}\right)\overline{u}_{\mathrm{m}} \tag{2}$$

In the model affected by the air volume, the ambient temperature T = 20 °C, and the table shows that the saturated vapor pressure and partial pressure P_{s} = 2337 Pa; when the pressure P = 101 325 Pa and the relative humidity φ = 0.6, the gas density formula is as follows

$$\rho = 0.003484\frac{P}{273 + T}\left(1 - \frac{0.378\varphi P_{\mathrm{s}}}{P}\right) \tag{3}$$

The air density is calculated to be 1.1985 kg/m^3. In the temperature influence model, since the change of air density has little influence on the wind speed distribution of the roadway, the influence of air temperature change on the wind speed distribution function is not considered, and the air density is calculated to be 1.1985 kg/m^3.

https://doi.org/10.1021/acsomega.3c06816
ACS Omega 2024, 9, 866−878

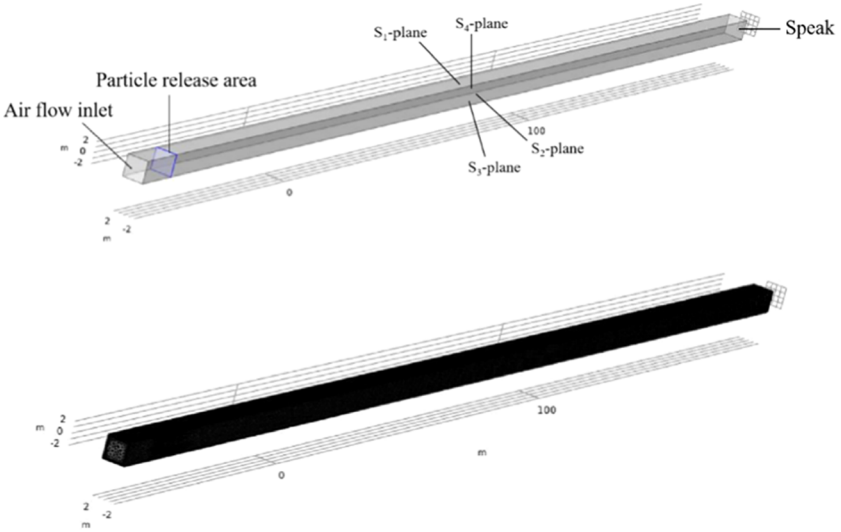

Figure 1. Geometric model and mesh division.

The wall of the wind inlet roadway in the Wulihou coal mine is concreted arch walling and plasterized outside. The value of $\alpha \times 10^4$ is 3×10^{-3} N·s^2·m^{-4} after investigation. Substitute r_0 = 2.8284 m, $\alpha = 3 \times 10^{-3}$ N·s^2·m^{-4}, and ρ = 1.1985 kg/m^3 into eq 2, and take roadway section as YZ plane and center as origin to obtain

$$\overline{u} = \left(0.8666 + 0.2502\sqrt{1 - \frac{\sqrt{y^2 + z^2}}{2.8284}}\right)\overline{u}_{\mathrm{m}} \tag{4}$$

The formula for calculating the average wind speed is

$$\overline{u}_{\mathrm{m}} = \frac{Q}{ab} \tag{5}$$

In the equation, Q is the air volume through the section, m^3/s; a is the section length of roadway, m; and b is the section height of the roadway, m.

2.3. Geometric Model. COMSOL software is used to establish a three-dimensional coordinate system through the practical measurement of the Wulihou coal mine's air inlet roadway. The calculation area of the model is a rectangular restricted space with a cross-sectional size of 4 m × 4 m and a length of 250 m. The particle release domain is 5 m away from the air inlet, and the thickness of the domain is 0.1 m. The geometric modeling and its mesh division are shown in Figure 1.

2.4. Simulation Scheme. For the air volume influence model, the main influencing factor is ventilation air volume, which is set as 40, 60, 80, 100, and 120 m^3/s, and the average wind speed corresponding to the air volume is 2.50, 3.75, 5.00, 6.25, and 7.50 m/s according to eq 5. Other parameters are set as shown in Table 1.

For the temperature influence model, the main influencing factor is air flow temperature. The initial temperature of air flow is set at 10, 15, 20, and 25 °C, and the temperature gradient is −0.03y, that is, the temperature drops by 3 °C every hundred meters into the roadway, and the ventilation air volume is 70 m^3/s, and the average wind speed is 4.375 m/s, as shown in eq 5. Other parameters are set as shown in Table 2.

Table 1. Air Volume Influence Model Parameters

model variable	parameter setting
turbulence model	standard k-ε
turbulence intensity	low
temperature/(°C)	20
air density/(kg/m^3)	1.1979
dust density/(kg·m^{-3})	2800
dust particle diameter/(μm)	1.0,3.5,7.5,15
the amount of dust released at each time/(grain)	100
release mode	random release
release time/(s)	0
wall condition	floor of roadway:freeze
	inlet/outlet:traverse
	wall of roadway:bounce
heat conduction	close
output time	range(0, 0.02, 120), range(0, 0.02, 80), range(0, 0.02, 60), range(0, 0.02, 50), range(0, 0.02, 40)

Table 2. Air Volume Influence Model Parameters

model variable	parameter setting
turbulence model	standard k-ε
turbulence intensity	low
temperature/(°C)	10, 15, 20, 25
temperature gradient	−0.03y
wind density/(kg·m^{-3})	1.2433, 1.2222, 1.1979, 1.1756
dust density/(kg·m^{-3})	2800
dust particle diameter/(μm)	1.0, 3.5, 7.5, 15
the amount of dust released at each time/(grain)	100
release mode	random release
release time/(s)	0
wall condition	floor of roadway:freeze
	inlet/outlet:traverse
	wall of roadway:bounce
heat conduction	open
output time	range (0, 0.02, 65)

https://doi.org/10.1021/acsomega.3c06816
ACS Omega 2024, 9, 866−878

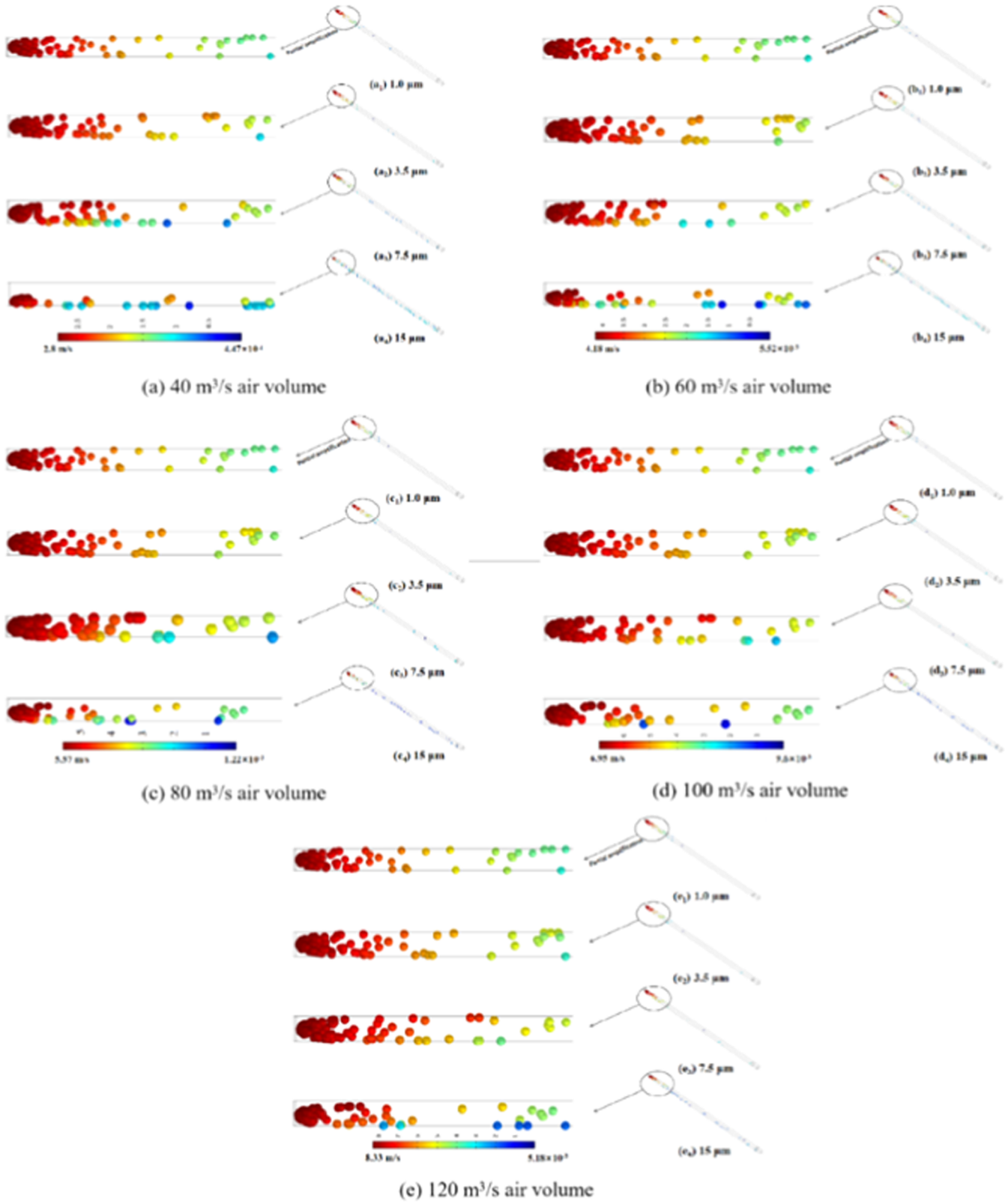

Figure 2. Movement results of dust in roadway under different air volumes.

3. RESULT AND ANALYSIS

3.1. Air Volume Influence. To simulate the movement of dust in air flow, the iterative calculation of air flow must be carried out first. After the air flow movement rule is obtained, the motion trajectory of dust with particle sizes of 1.0, 3.5, 7.5, and 15 μm under five kinds of air flow is studied by COMSOL numerical simulation software. Under the same air volume, the time of dust with different particle sizes arriving at the roadway exit is basically the same. In the process of dust movement, the screenshots of the first particle arriving at the roadway exit are presented as simulation results, as shown in Figure 2, and the

https://doi.org/10.1021/acsomega.3c06816
ACS Omega 2024, 9, 866−878

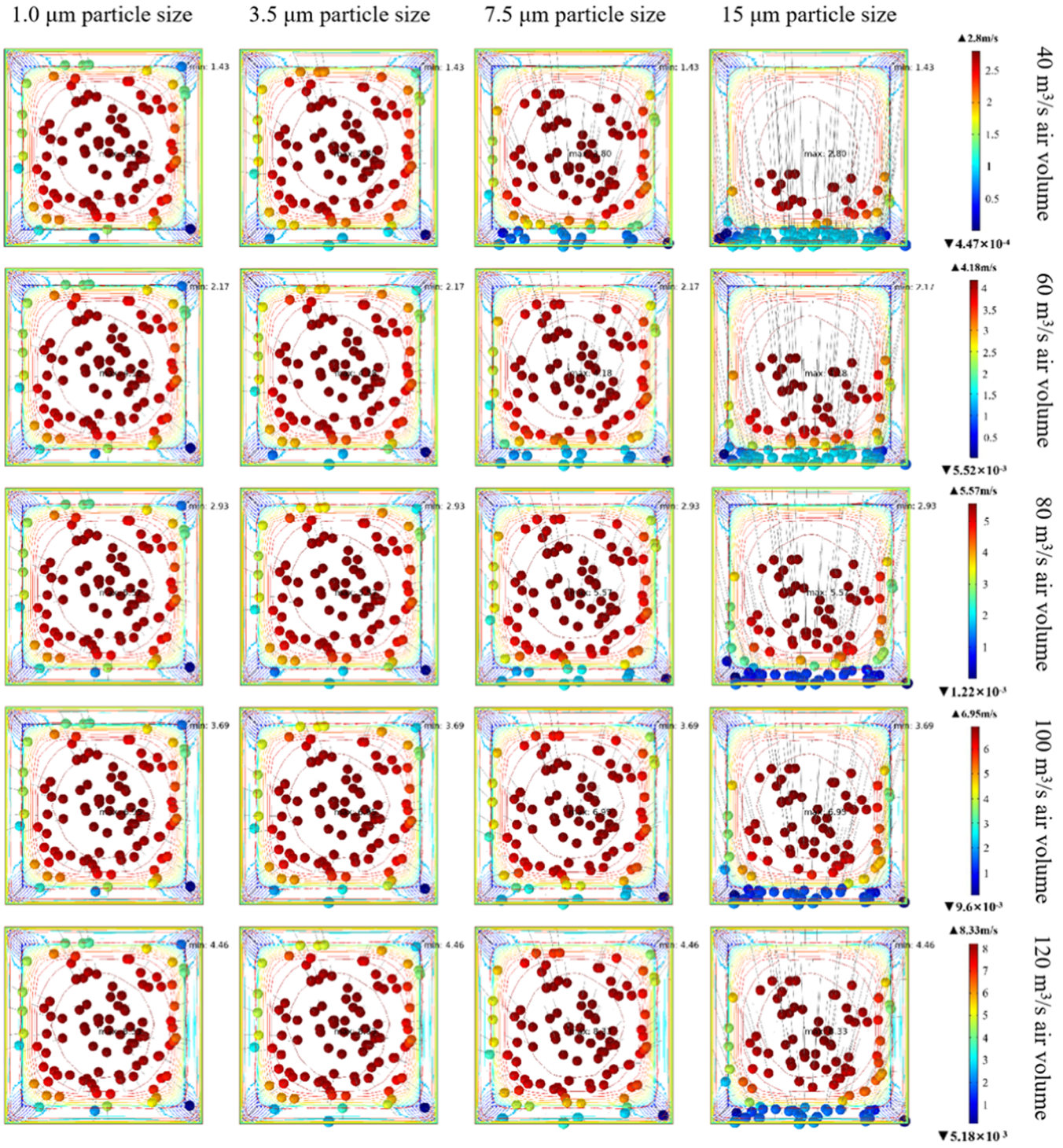

Figure 3. Contour map of dust final velocity.

Table 3. Falling Height of Dust at the Exit of the Roadway/m

		diameter (μm)			
ventilation ($m^3 \cdot s^{-1}$)	time (s)	1.0	3.5	7.5	15
40	86.48	0.0021	0.1283	0.6257	2.0000
60	57.82	0.0012	0.0828	0.4153	1.6985
80	43.42	−0.0036	0.0603	0.3100	1.2706
100	34.78	−0.0046	0.0467	0.2466	1.0152
120	29.00	−0.0050	0.0377	0.2045	0.8447

obtained data are taken as the movement results of dust with this particle size under corresponding air volume.

In the simulation results, the final velocity of dust with different particle sizes is shown in Figure 3, where the annular line represents the velocity contour line.

As can be seen from Figure 2, under the same ventilation volume, dust with particle sizes of 1.0, 3.5, and 7.5 μm has little change in the height of the spatial concentration, but dust with particle sizes of 15 μm has obvious subsidence. The color example increases with the increase of the air volume, particles with the lowest velocity settle at the bottom of the roadway,

https://doi.org/10.1021/acsomega.3c06816
ACS Omega 2024, 9, 866−878

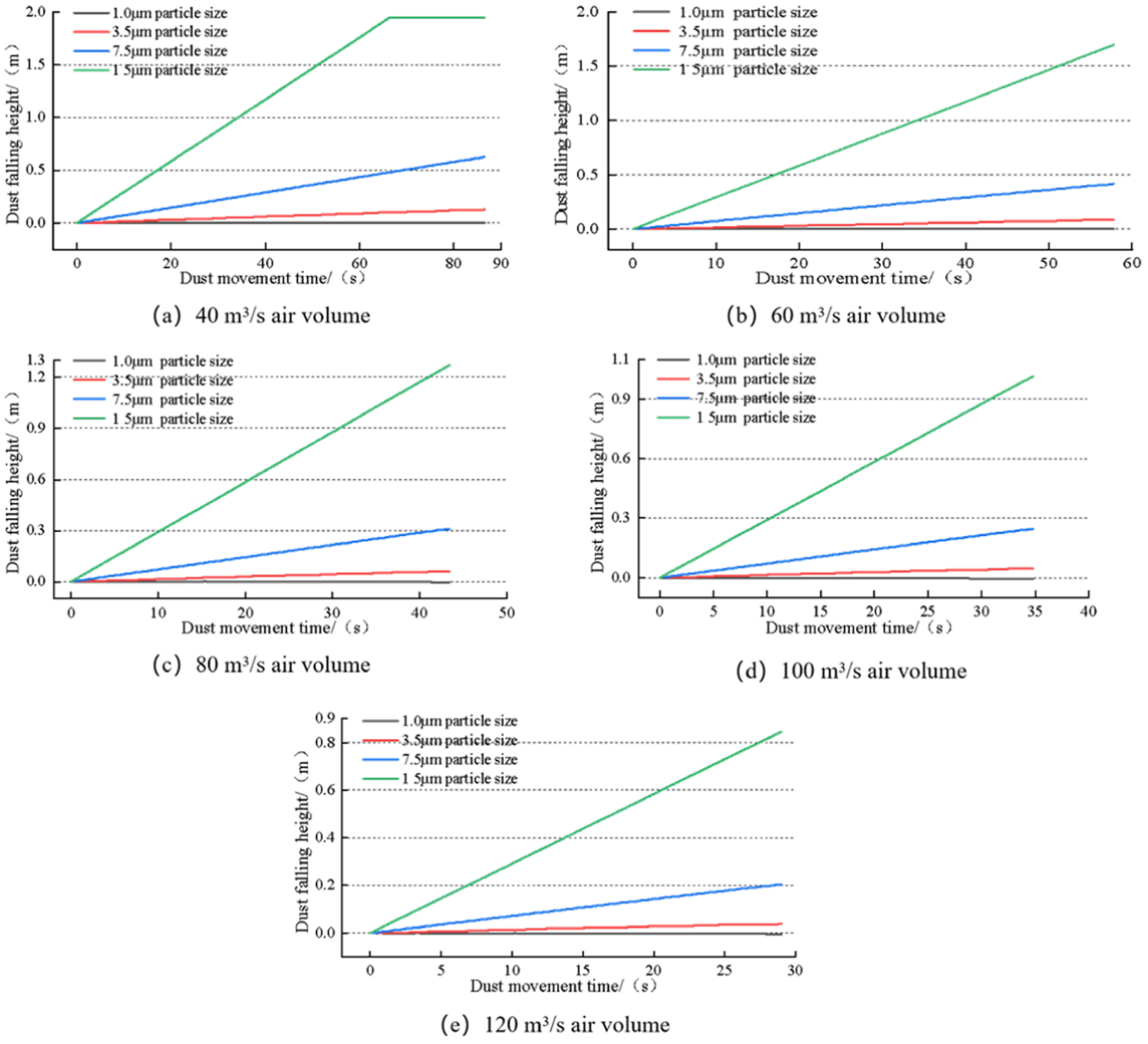

Figure 4. Dropping height of dust with different particle sizes at the same air volume.

and the amount of sedimentation increases with the increase of dust particle size. The horizontal comparison in Figure 3 shows that the highest dust velocity is concentrated in the center of the roadway, and its velocity decreases radially from the center to the periphery. The highest volume air volume is on the axis line of the roadway, and the lowest volume air volume is on the upper right corner of the roadway, which is consistent with the distribution law of wind speed in the roadway section. Under the same ventilation volume, the larger the dust particle size, the more obvious the settlement and the higher the proportion of low-speed dust. Through the longitudinal comparison, it can be seen that the larger the particle size, the more obvious the influence of air volume on the particle size dust, but the influence of air volume on its spatial coordinates is still small.

Dust O_1 ($y = -0.0174$, $z = 0.0283$) released closest to the roadway center is taken as the object of analysis. The falling height of the dust at the roadway exit is shown in Table 3. The negative value in the table indicates that the dust particle is above the initial horizontal position when it reaches the roadway exit (the same as below).

Under the condition of the same air volume, the falling height of dust with different particle sizes in the whole roadway changes with time, as shown in Figure 4.

In the force of dust, the vertical force includes the resultant force of gravity and buoyancy, the Saffman lift force, and the pressure gradient force. Because the main direction of drag force is opposite to the direction of dust movement, the falling height of dust in the vertical direction changes little over time, so the drag force of dust in the vertical direction can be ignored. Let the net force in the vertical direction be F-compound and positive downward. As can be seen from Table 3, when the ventilation volume reaches 80 m^3/s, the falling height of dust with a particle size of 1.0 μm begins to appear negative. Therefore, the phenomenon of dust rising appears in the simulation. The direction of F-cohesion received by dust is upward, that is, the upward resultant force is greater than the downward resultant force. From Figure 4(a–e), it can be seen

https://doi.org/10.1021/acsomega.3c06816
ACS Omega 2024, 9, 866–878

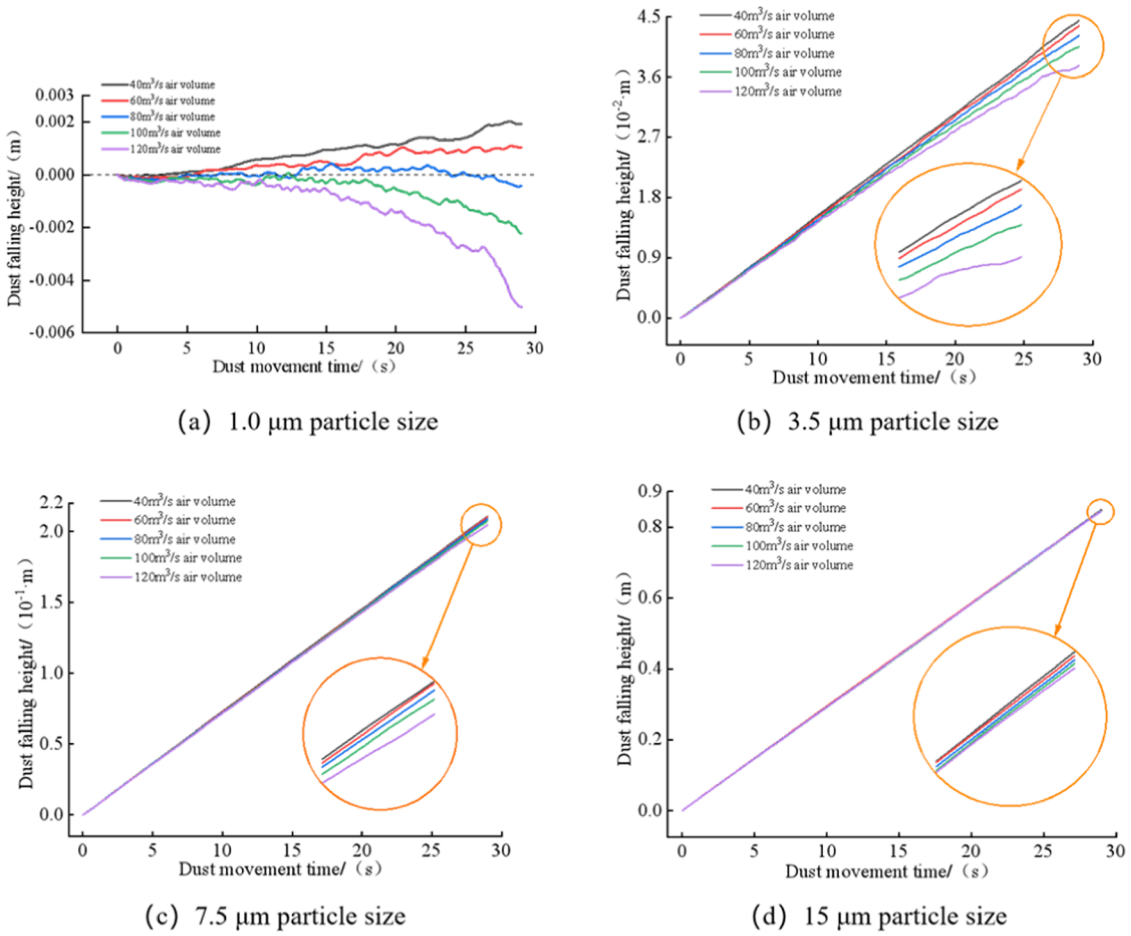

Figure 5. Falling height of dust at different air volumes.

that under the condition of the same ventilation volume, dust with different particle sizes takes the same time to arrive at the exit of the roadway. Figure 4(a) shows that when the ventilation volume is 40 m^3/s, dust with a particle size of 15 μm settles to the bottom of the roadway after a movement of 66.16 s. Dust with other particle sizes is in suspension state before the end of the simulation; that is, it moves with the wind flow in the roadway. It can be seen from Figure 4 that under the same air volume, with the increase of dust particle size, the falling height when dust reaches the roadway exit increases. Therefore, the falling height when dust reaches the roadway exit is positively correlated to its particle size.

In the simulation results, when the air volume is 120 m^3/s, the dust movement duration is the shortest, which is 29 s. The falling height of the O_1 particle 29 s before the movement is shown in Figure 5.

As can be seen from Figure 5, with the increase of dust particle size, dust movement is less affected by the change of wind volume, dust movement trajectory tends to be consistent, and the smaller the particle size, the more obvious the influence of wind flow is. For dust with large particle size, the influence of other forces is far less than that of gravity on dust movement. For dust with small particle size, the influence of other forces is more obvious. Gravity no longer plays a decisive role in its falling process, but is more influenced by other forces and turbulence. As can be seen from Figure 5(a), within the set ventilation volume range, only dust with a particle size of 1.0 μm appears upward. When the ventilation volume is greater than 80 m^3/s, dust with a particle size of 1.0 μm receives an upward direction of F-compound, that is, the upward resultant force is greater than the downward resultant force. It can be seen from Figure 5(b–d) that when dust particle size is the same, dust falling height is negatively correlated with ventilation volume during the same movement time.

In summary, it can be concluded from the air volume influence model that when the ventilation air volume is the same, the falling height of dust reaching the outlet of the roadway is positively correlated to its particle size. With the increase of the dust particle size, the influence of the change of air volume on dust movement decreases, and the dust movement trajectory gradually tends to be consistent. When the dust particle size is the same, the dust falling height is negatively correlated to the ventilation volume during the same movement time.

3.2. Temperature Influence. In the process of dust movement, the screenshot when the first dust reaches the exit of the roadway is presented as the simulation result, as shown in Figure 6.

When the initial air flow temperature is 25 °C, the dust movement time is the shortest, which is 49.30 s. The movement data of 49.30 s before dust in the temperature influence model is used for analysis, and the dust O2 (y = −0.1833, z = −0.1767) released closest to the roadway center is taken as the analysis object. The falling height of the dust at the exit of the roadway is shown in Table 4. The negative value in the table indicates that the dust particle is above the initial

https://doi.org/10.1021/acsomega.3c06816
ACS Omega 2024, 9, 866−878

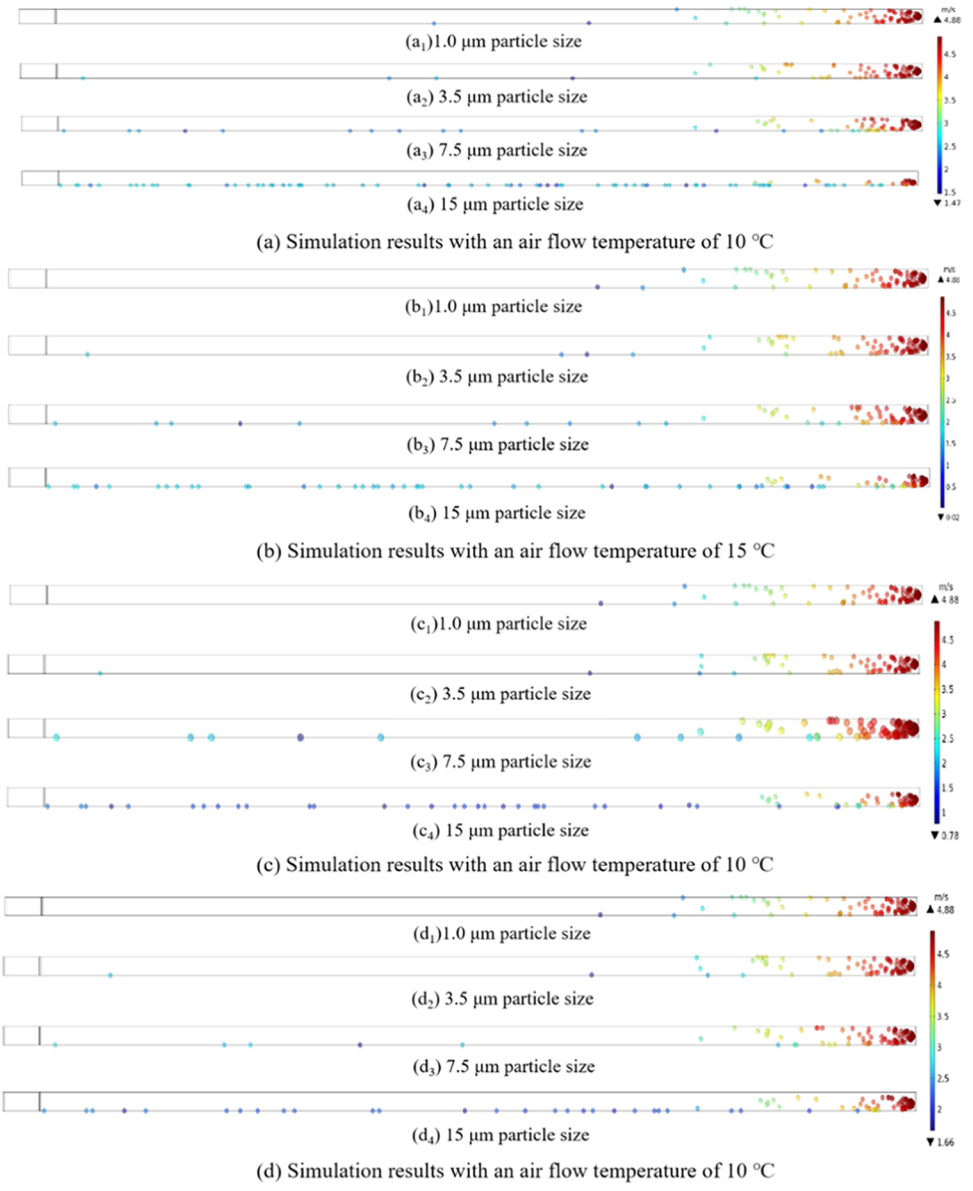

Figure 6. Simulation results at different air flow temperatures.

Table 4. Falling Height of Dust at 49.30 s/10^{-2}·m

	initial temperature of wind (°C)			
dust diameter (μm)	10	15	20	25
1.0	−0.232	−0.250	−0.274	−0.303
3.5	0.486	0.464	0.437	0.405
7.5	1.322	1.298	1.265	1.225
15	2.151	2.119	2.078	2.025

Table 5. Effect of Temperature on Dust Fall Height at the Same Time

diameter (μm)	dust falls high at 10 °C (10^{-2}·m)	dust falls high at 25 °C (10^{-2}·m)	range (10^{-2}·m)	maximum impact rate (%)
1.0	−0.232	−0.303	0.071	30.60
3.5	0.486	0.405	0.081	16.67
7.5	1.322	1.225	0.097	7.34
15	2.151	2.025	0.126	5.86

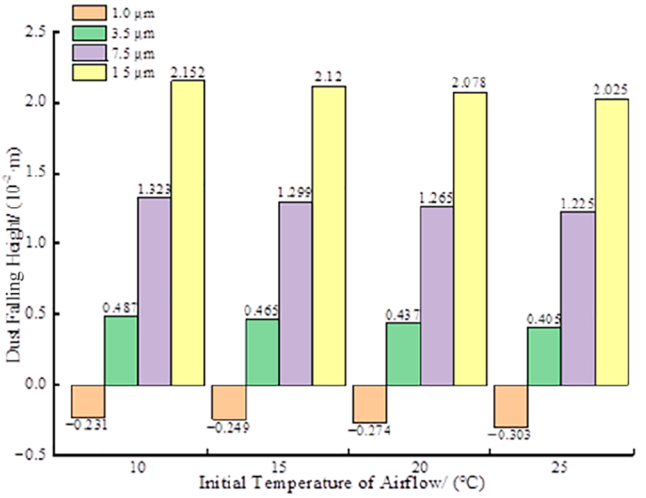

Figure 7. Dust falling height at different temperatures.

https://doi.org/10.1021/acsomega.3c06816
ACS Omega 2024, 9, 866−878

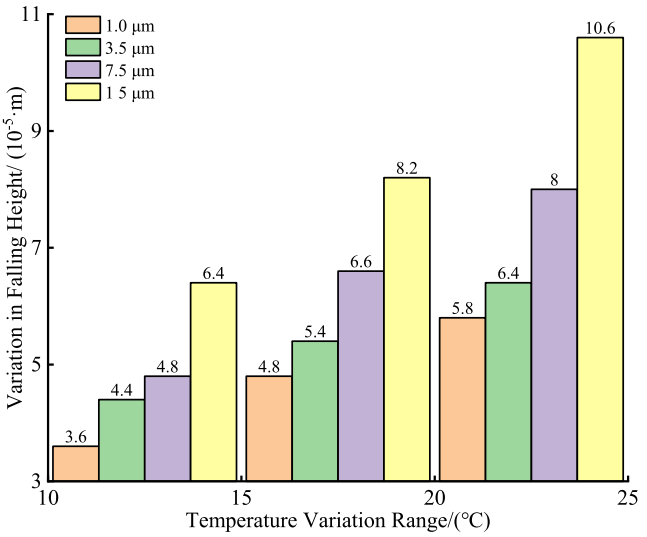

Figure 8. Relationship between gas concentration and dust suspension ratio in roadways.

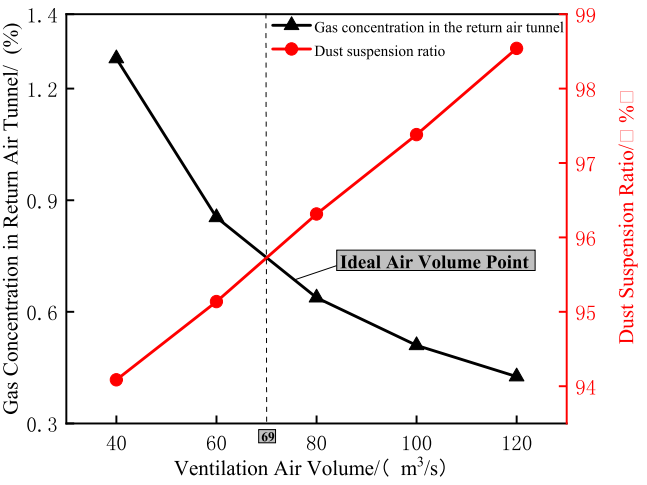

Figure 9. Relationship between gas concentration and dust suspension ratio in roadways.

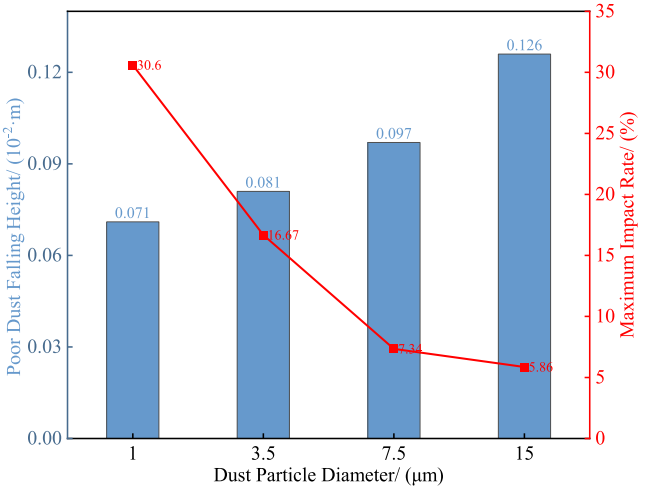

Figure 10. Settling quantity and proportion of actual mixed dust.

position when it reaches the exit of the roadway, and the value represents the vertical moving distance.

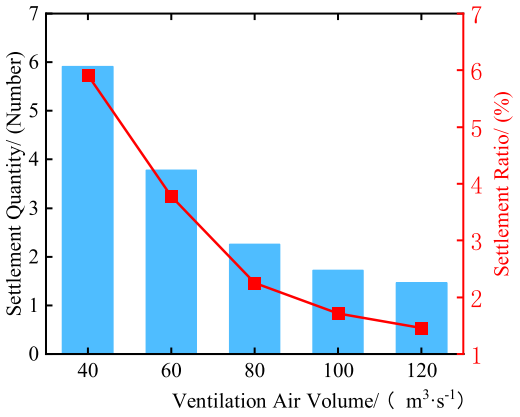

Figure 11. Effect of temperature on the falling height of dust with different particle sizes.

As can be seen from Table 4, during the same movement time, the falling height of dust with the same particle size is negatively correlated with the initial temperature of air flow. At the same air flow temperature, the falling height of dust is positively correlated to its particle size. From the variation range of data, it can be seen that dust particle size has a greater impact on its falling height than the air flow temperature.

In Table 4, dust with the same particle size has the smallest falling height at 25 °C and the largest falling height at 10 °C. The absolute value of the difference between the falling height of dust at 10 and 25 °C is defined as the range of falling height of dust with this particle size. By dividing the range by the absolute value of falling height of dust at 10 °C, the maximum influence rate of temperature on its movement can be obtained. As shown in Table 5.

Dust falling height at different temperatures is shown in Figure 7 and 8.

By comparing the data of different particle sizes of dust in Figures 5−24, it can be concluded that when the dust particle size is the same, as the air flow temperature increases, the change in dust drop height caused by the unit temperature change increases. Therefore, the change in dust drop height caused by unit temperature change is positively correlated with the air flow temperature because the higher the temperature, the higher the relative energy in the system. Based on the conclusion that the falling height of dust with the same particle size in the tunnel is negatively correlated with the air flow temperature, it can be concluded that as the air flow temperature increases, the dust suspension becomes more pronounced, which is not conducive to dust reduction in the intake tunnel.

The height of particles falling in the simulation results is shown in the figure, with column height indicating the dust falling height and negative values indicating dust rising. For dust with the same particle size, the higher the temperature, the smaller the height of dust falling during movement, and the height of dust falling is negatively correlated with the air flow temperature. This indicates that the higher the temperature, the longer the suspension time of dust and the greater its impact on subsequent places, which is not conducive to the improvement of the tunnel environment.

The relationship between the gas concentration and dust suspension ratio in roadways is shown in Figure 9.

From Figure 9, it can be concluded that the optimal ventilation air volume is 69 m^3/s without additional dust

https://doi.org/10.1021/acsomega.3c06816
ACS Omega 2024, 9, 866−878

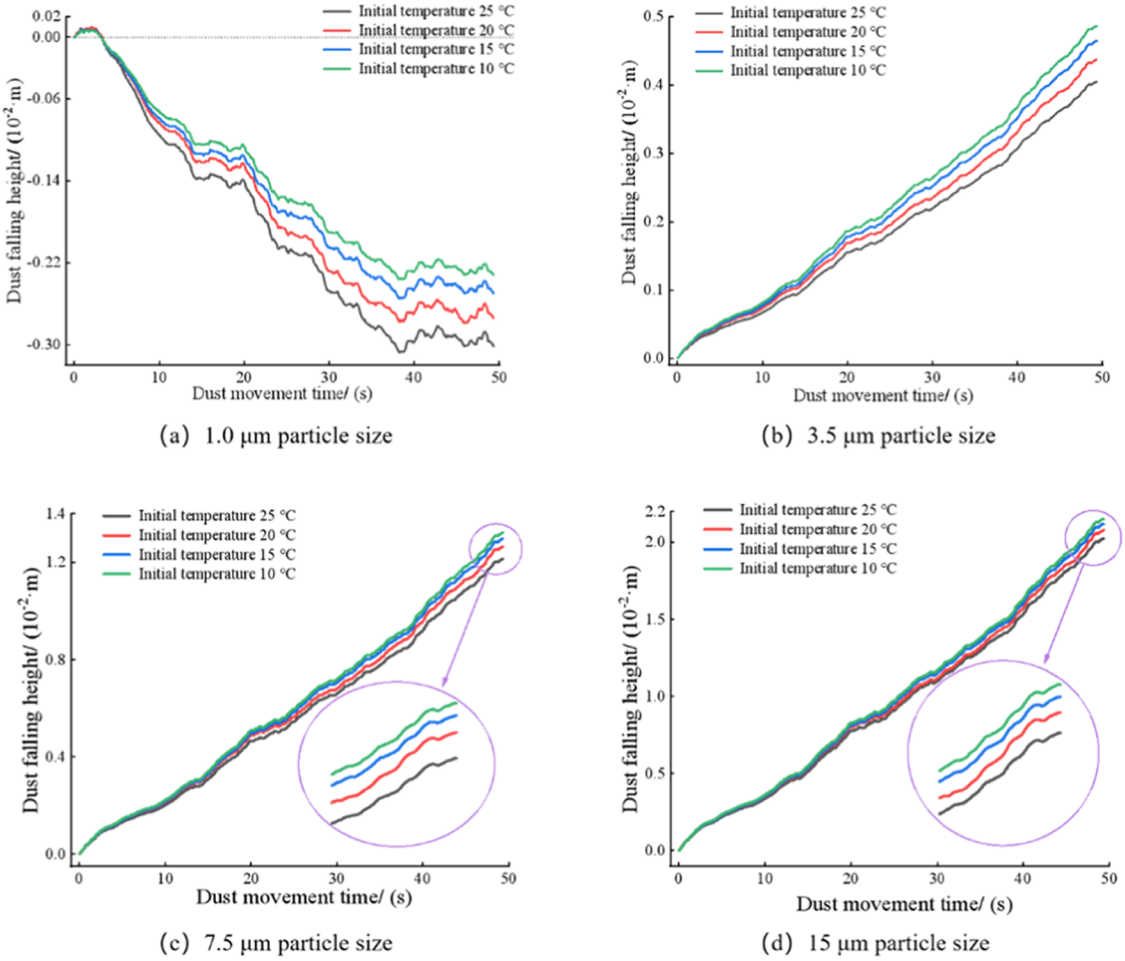

Figure 12. Falling height of dust with the same particle size at different temperatures.

removal devices in the main air inlet of the Wulihou Coal Mine. According to the Coal Mine Safety Regulations, the gas concentration in the total return air flow of the mine does not exceed 0.75%. When the main air inlet air volume is 69 m^3/s, the corresponding gas concentration in the return air flow should be 0.741%, meeting the requirements of the Coal Mine Safety Regulations.

The influence degree of temperature on dust falling height of different particle sizes is shown in Figure 10. Column height represents the range of dust falling height, that is, the difference of dust falling height between 25 and 10 °C; the broken line represents the maximum influence rate of temperature on dust.

As can be seen from Figure 10, with the increase of dust particle size, the range of dust falling height becomes larger, but the maximum influence rate of temperature on dust gradually decreases; that is, the influence of air flow temperature on dust movement characteristics is weakened. Therefore, the influence degree of air flow temperature on dust movement is negatively correlated with dust particle size. This is because the larger the particle size of dust, the more it is affected by gravity, and the smaller the particle size, the more obviously it is affected by other forces and turbulence.

As can be seen from Figure 11, the actual settlement amount of dust in the tunnel is 5.913%. The same method can be used to obtain an actual dust settling rate of 3.783% when the air volume is 60 m^3/s. The actual settling rate of dust is 2.250% when the air volume is 80 m^3/s. The actual settling rate of dust is 1.718% when the air volume is 100 m^3/s. The actual settling rate of dust is 1.460% when the air volume is 120 m^3/s.

The falling height of dust with the same particle size under different air temperatures is shown in Figure 12.

Observed from the direction of the tunnel exit, the density accumulation of dust with a particle size of 15 μm under different air flow temperatures is shown in Figure 13.

As can be seen from Figure 12(a), dust with a particle size of 1.0 μm has an upward trend in air flow at different temperatures, and the upward trend of dust is more significant as the air flow temperature increases. From Figure 12(b–d), it can be seen that the larger the particle size, the higher the dust falling height, and the dust moving trajectory tends to be consistent gradually. In Figure 10, with the decrease of the air flow temperature, the height of density accumulation of dust gradually decreases and the center of gravity of density accumulation gradually moves down. By combining the analysis of Figures 12 and 13, it can be concluded that for dust with the same particle size, the higher the temperature, the smaller the falling height of dust will be in the process of movement. Therefore, the falling height of dust is negatively correlated with the air flow temperature. The higher the temperature, the longer the dust stays in suspension state and the worse the roadway environment. Under the condition that other factors remain unchanged, the roadway environment at night should be better than during the day, and winter should be better than summer. In the roadway system, the higher the

https://doi.org/10.1021/acsomega.3c06816
ACS Omega 2024, 9, 866−878

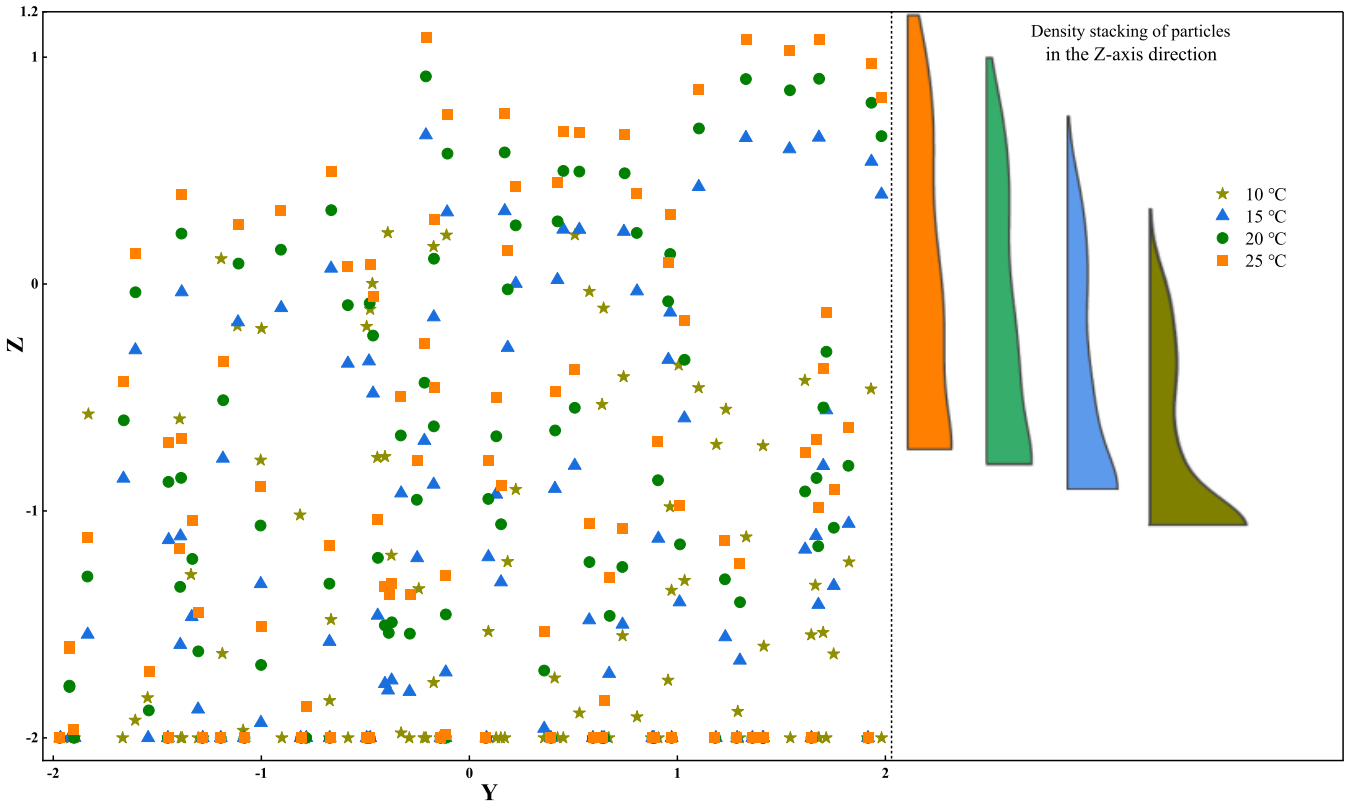

Figure 13. Density accumulation of dust with a particle size of 15 μm at different air flow temperatures.

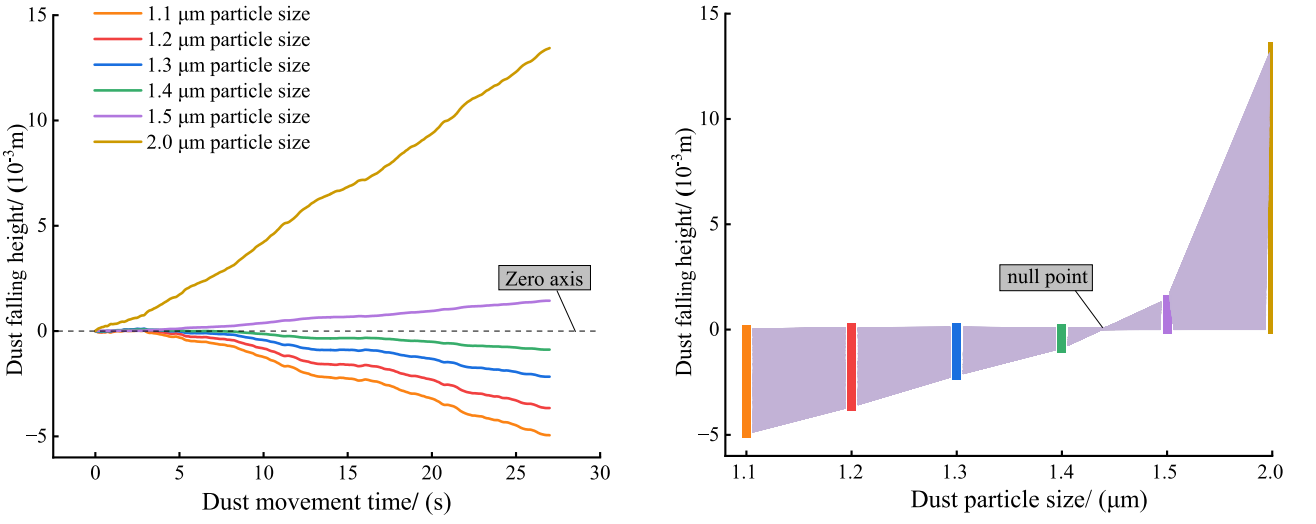

(a)The relationship between dust movement time and falling height (b)The relationship between dust particle size and falling height

Figure 14. Falling height of dust with different particle sizes in 27 s when the air volume is 128 m^3/s. Falling height of dust with a particle size of 1.0 μm moving for 29 s at different air volumes.

temperature, the higher the relative energy, the higher the entropy inside the system, and the more intense the molecular movement. Since entropy is mainly used for macroscopic objects, the less the dust is affected by external forces, so the settlement under gravity will be relatively slowed down, but this influence is limited. Therefore, the falling height of large particle size dust in the roadway at higher temperatures is still much higher than that of small particle size dust in the roadway at lower temperatures.

3.3. Dust Analysis. As can be seen from Table 3, the critical ventilation volume of dust is within 60−80 m^3/s. The particle size of the dust was set to 1.0 μm for simulation, and the O_3(y = 0.0256, z = −0.0590) particles close to the release center were taken as the analysis object. The dichotomy method was used to determine the critical air volume that could make the dust rise within 75−80 m^3/s. Within the selected air volume range, the falling height of the dust movement for 29 s is shown in Figure 14.

As can be seen from Figure 14(a), when the air volume is 76 m^3/s, 1.0 μm particle size dust begins to rise. As can be seen from Figure 14(b), the critical air volume for the rise of the O_3 particles ranges from 75 to 76 m^3/s, so the minimum air

https://doi.org/10.1021/acsomega.3c06816
ACS Omega 2024, 9, 866−878

volume for the rise of the O_3 particles is 76 m^3/s. According to eq 5, the average wind speed of the roadway is $\overline{u}_m$ = 4.75 m/s. The coordinates and $\overline{u}_m$ = 4.75 m/s of the particle in the roadway section are substituted into eq 4 to obtain $\overline{u}$ = 5.29 m/s. Then, y = 0, z = 0, and $\overline{u}$ = 5.29 m/s are substituted into eq 4 to obtain the average wind speed of the roadway $\overline{u}_m$ = 4.74 m/s. Substituting the average wind speed and the length and width of the roadway into eq 5, Q = 75.84 m^3/s is obtained. Therefore, the critical air volume for dust rising in the roadway is 75.84 m^3/s, and the corresponding wind speed in the center of the roadway is 5.29 m/s.

According to the Coal Mine Safety Regulations, the average wind speed of the inlet tunnel shall not exceed 8 m/s, so the maximum inlet air volume of the Wulihou coal mine is 128 m^3/s, and the ventilation air volume is set as 128 m^3/s for simulation. O_4 particles (y = 0.0143, z = 0.0997) are taken as the analysis object. The dichotomy method was used to find that the critical particle size of the dust rising was between 1.0 and 1.5 μm. Within the selected particle size range, the falling height of dust at 27 s is shown in Figure 14.

As can be seen from Figure 14(a), under the maximum allowable air volume, the particle size of the particle of the O_4 starts to rise when it is less than 1.5 μm. As can be seen from Figure 14(b), the critical particle size of the O_4 particle is within 1.4−1.5 μm. Therefore, within the permissible range, the critical particle size of dust rising in this roadway is 1.4 μm. Therefore, dust with a particle size greater than 1.4 μm will settle. Regardless of the factors of roadway length and time, this part of dust will eventually settle to the bottom of the roadway.

To sum up, the critical air volume of dust in this roadway is 75.84 m^3/s, and the corresponding wind speed in the center of the roadway is 5.29 m/s. The critical particle size of dust generation is 1.4 μm.

4. CONCLUSIONS

Through numerical simulation of the dust movement process in the intake tunnel of the Wulihou Coal Mine, the following conclusions were obtained:

(1) In the inlet roadway, when the ventilation air volume is the same, the falling height of dust reaching the outlet of the roadway is positively correlated with its particle size. When the dust particle size is the same, the dust falling height is negatively correlated with the ventilation volume during the same movement time. With the increase of dust particle size, the influence of the change of wind volume on its movement decreases, and the dust movement trajectory gradually tends to be consistent. Therefore, increasing the ventilation air volume in the tunnel is not conducive to dust reduction.

(2) The falling height of dust is negatively correlated with the air flow temperature. Under the condition that other factors remain unchanged, the environment in the roadway at night should be better than in the daytime, and winter better than in summer. Therefore, increasing the ventilation air volume in the tunnel is not conducive to dust reduction.

(3) Therefore, increasing the ventilation air volume in the tunnel is not conducive to dust reduction: the critical air volume of dust in the inlet tunnel is 75.84 m^3/s, and the corresponding wind speed in the center of the tunnel is 5.29 m/s. The critical particle size of dust is 1.4 μm.

AUTHOR INFORMATION

Corresponding Authors

YeMing Zhu − *Department of Nuclear Emergency and Nuclear Safety, China Institute for Radiation Protection, Taiyuan 030006 Shanxi, China*; orcid.org/0009-0007-4352-2182; Email: 11804010@qq.com

ShuTang Sun − *Department of Nuclear Emergency and Nuclear Safety, China Institute for Radiation Protection, Taiyuan 030006 Shanxi, China*; Email: sunshutang@126.com

Authors

Tao Chen − *College of Safety and Emergency Management Engineering, Taiyuan University of Technology, Taiyuan 030024 Shanxi, China*

Ying Ji − *Taiyuan Power Supply Company, State Grid Shanxi Electric Power Company, Taiyuan 030001 Shanxi, China*

Dong Zhao − *College of Safety and Emergency Management Engineering, Taiyuan University of Technology, Taiyuan 030024 Shanxi, China*

DaJie Zhuang − *Department of Nuclear Emergency and Nuclear Safety, China Institute for Radiation Protection, Taiyuan 030006 Shanxi, China*

YiRen Lian − *Department of Nuclear Emergency and Nuclear Safety, China Institute for Radiation Protection, Taiyuan 030006 Shanxi, China*

Yu Rong − *Department of Nuclear Emergency and Nuclear Safety, China Institute for Radiation Protection, Taiyuan 030006 Shanxi, China*

Jin Yan − *Department of Nuclear Emergency and Nuclear Safety, China Institute for Radiation Protection, Taiyuan 030006 Shanxi, China*

HongChao Sun − *Department of Nuclear Emergency and Nuclear Safety, China Institute for Radiation Protection, Taiyuan 030006 Shanxi, China*

Complete contact information is available at: https://pubs.acs.org/10.1021/acsomega.3c06816

Notes

The authors declare no competing financial interest.

ACKNOWLEDGMENTS

The Research Project was supported by Shanxi Scholarship Council of China (grant no. 2022-052) and Science and Technology Innovation Project of University of Shanxi Province in China (grant no. 20200075). Thanks go to Zhao Dong for his feedback and suggestions from the beginning of the topic selection to the end of the final draft. The authors express their high respect and sincere gratitude to Teacher Zhao Dong and thank Senior Brother Chen Tao for help in simulating this article. They also thank Ji Ying for support in the creation of this paper.

REFERENCES

(1) Cui, D. Research Progress of Dust Movement and Diffusion Laws in Excavation Roadway *Safety Coal Mines* 2018.

(2) Yuan, L. Scientific conception of coal mine dust control and occupational safety. *J. China Coal Soc.* **2020**, *45* (1), 1−7.

(3) Liu, S.; Li, X. Experimental study on the effect of cold soaking with liquid nitrogen on the coal chemical and microstructural characteristics. *Environ. Sci. Pollut. Res.* **2023**, *30* (13), 36080−36097.

(4) Li, X.; Cao, Z.; Xu, Y. Characteristics and trends of coal mine safety development. *Energy Sources, Part A* **2021**, 1−9.

https://doi.org/10.1021/acsomega.3c06816
ACS Omega 2024, 9, 866−878

(5) Liu, S.; Sun, H.; Zhang, D.; Yang, K.; Li, X.; Wang, D.; Li, Y. Experimental study of effect of liquid nitrogen cold soaking on coal pore structure and fractal characteristics. *Energy* **2023**, *275*, No. 127470.
(6) Liu, H.; Li, X.; Yu, Z.; Tan, Y.; Ding, Y.; Chen, D.; Wang, T. Influence of hole diameter on mechanical properties and stability of granite rock surrounding tunnels. *Phys. Fluids* **2023**, *35* (6), No. 064121.
(7) Zhang, J.; Li, X.; Qin, Q.; et al. Study on overlying strata movement patterns and mechanisms in super?large mining height stopes. *Bull. Eng. Geol. Environ.* **2023**, *82* (4), No. 142.
(8) Ma, Q.; Nie, W.; Yang, S.; et al. Effect of spraying on coal dust diffusion in a coal mine based on a numerical simulation. *Environ. Pollut.* **2020**, *264* (2), No. 114717.
(9) Ren, W.; Wang, D.; Guo, Q.; Zuo, B. Application of foam technology for dust control in underground coal mine. *Int. J. Min. Sci. Technol.* **2014**, *24* (1), 13−16.
(10) Zheng, H.; Jiang, B.; Zheng, Y.; et al. Experimental study on forced ventilation and dust-control in a heading face based on response surface method. *Process Saf. Environ. Prot.* **2023**, *175*, 753−763.
(11) Mo, J.; Ma, W. Researches on the numerical simulation of the dust pollution characteristics and the optimal dust suppression wind-speed on fully mechanized caving face. *Energy Explor. Exploit.* **2022**, *40* (2), 800−815.
(12) Tallón-Ballesteros, A. J. Numerical Simulation Study of Dust Transport of Comprehensive Mining Working Surface. *Modern Management Based on Big Data III: Proceedings of MMBD* **2022**, *352*, 440.
(13) Wang, J. *Research on Dust Migration and Settlement Characteristics in the Return Airway Wind Flow of Coal Mining Face*; China University of Mining and Technology, 2017.
(14) Zhou, G.; Yin, W.-J.; Feng, B. Numerical simulation on the distribution characteristics of dust-droplet field during support movement in a fully-mechanized mining face and related engi-neering applications. *China Coal Soc.* **2018**, *43* (12), 3425−3435.
(15) Jiang, Z.-A.; Gao, K.-N.; Chen, J.-H.Dust distribution rule and influencing factors in mobile grinding operation *J. Cent. South Univ. (Sci. Technol.)* 2019; Vol. *50* 5, pp 1028−1034.
(16) Hu, S.-Y.; Liao, Q.; Wang, H.-T.; Feng, G.-R.; Xu, L.-H.; Huang, Y.-S.; Shao, H.; Gao, Y.; Hu, F. Gas-solid two-phase flow at high-gassy fully mechanized within high gassy coal seam. *J. China Coal Soc.* **2019**, *44* (12), 3921−3930.
(17) Wang, M.Similar simulation study on the flow field structure and the law of dust settlement of heading roadway *Min. Saf. Environ. Prot.* 2021; Vol. *48* 03, pp 56−61.
(18) Deji, J. I.; Dening, W. E.; Mingxing, M. A.; Tian, Z. H.; Xiangxi, M. E.; Shuaishuai, R. E. Study on dust movement in belt transportation roadway and pneumatic spray dust control technology. *China Saf. Sci. J.* **2021**, *31* (11), 93−99.
(19) Guo, Y.-F.; Hao, Y.-J.; Li, Y.-L.; Guo, W.-Q.Dust diffusion and migration law of transferring and crushing point in fully mechanized coal caving face *Coal Eng.* 2022; Vol. *54* 02, pp 73−77.
(20) Ma, S.-L.; Zhang, Q.; Gong, X.-Y.Research on dust prevention and control of door-type air curtain dust control and removal system in fully mechanized excavation face *Min. Saf. Environ. Prot.* 2022; Vol. *49* 2, pp 16−20.
(21) Li, Y.-C.; Li, Z.; Gao, L. Arrangement of air duct in tunneling working face based on the distribution laws of airflow and dust. *J. China Coal Soc.* **2014**, *39* (1), 130−135.
(22) Zhang, J.-J. *Gas-Solid Two-Phase Flow Simulation of Dust Migration and Deposition in Fully Mechanized Heading Face*; China University of Mining and Technology, 2015.
(23) Xu, M.-Y. *Research of Dust Movement in Roadway and Pipeline Deposition Law in Extractable Ventilation*; China Coal Research Institute, 2018.
(24) Gong, J. *Research on the Movement Regularities of Dust and Ventilation System Optimization in Excavation Face of High-altitude Mine*; University of Science and Technology Beijing, 2016.
(25) John, D.; Anderson, J. R. Computational Fluid Dynamics: The Basics with Applications Tsinghua University press, 2010.
(26) Chen, S.-J.; Qi, Y.-G.; Li, G.-G.Study on dust suspension law in driving roadway with forced ventilation *Safety Coal Mines* 2022; Vol. *53* 04, pp 178−182.
(27) Ji, C. S. The distribution function of turbulent velocity in pipe flow. *China Mine Eng.* **2013**, *42* (4), 63−67.
(28) Chaosong, J. The Theoretical Foundation of Ventilation Process in Tunnel. *China Mine Eng.* **2005**, *34* (3), 32−34.
(29) Zhang, G.-S. *Ventilation Safety*; China University of Mining and Technology press, 2011.

https://doi.org/10.1021/acsomega.3c06816
ACS Omega 2024, 9, 866−878